Study of DVCS with HERA I and HERA II data

Summer Student Program 2008, DESY

Stefania Stucci

Universitá della Calabria

16th September 2008

This report describes the analysis of the DVCS process with the data collected by ZEUS during HERA I running period and a first look to the HERA II data.

Contents

1 Introduction **3**

2 Experimental set-up and Monte Carlo simulations **3**

3 Kinematic variables and event selection **5**

4 Background study and signal extraction **7**

5 Results **8**

6 Conclusion and Outlook **9**

7 Acknowledgements **10**

1 Introduction

This report presents the measurement of the cross section for the exclusive production of a real photon in diffractive positron[1]-proton interactions, $ep \rightarrow e\gamma p$, a process known as Deeply Virtual Compton Scattering (DVCS). In perturbative QCD, this process is described by the exchange of two partons, with different longitudinal and transverse momenta in a colourless configuration. At the $\gamma^* p$ centre-of-mass energies, W, available for ep collisions at the HERA collider, for large squared momentum transfer at the lepton vertex, Q^2, the DVCS process is dominated by two-gluon exchange. Measurements of the DVCS cross section provide constraints on the generalised parton distributions (GPDs) [1–5], which carry information about about the transverse distribution of partons in the proton which is not accessible through the measurements of the F_2 structure function. The simplicity of the final state and the absence of hadronisation effects mean that the QCD predictions for DVCS are expected to be more reliable than for exclusive vector meson production which has been extensively studied in ep collisions at HERA [6–13].

The report presents the measurement of the DVCS cross sections in the kinematic range of $1.5 < Q^2 < 100\,\text{GeV}^2$ and $40 < W < 170\,\text{GeV}$ for HERA I[2], $5 < Q^2 < 100\,\text{GeV}^2$ and $40 < W < 170\,\text{GeV}$ for HERA II. The study based on the HERA I data sample repeats a ZEUS analysis, presently being published, using and independent ROOT/C++-based analysis code. The HERA II analysis is a first feasibility study of the measurement of the DVCS cross section with selection criteria similar to the HERA I analysis. In order to make a comparison between the HERA I and the HERA II results an analysis was made applying the same cuts used for HERA II to the HERA I sample.

2 Experimental set-up and Monte Carlo simulations

The data used for this measurement, corresponding to an integrated luminosity of 61.1^{-1} for HERA I and 141.21 pb^{-1} for HERA II, were taken with the ZEUS detector when HERA collided positrons of 27.5 GeV with protons of 920 GeV. A detailed description of the ZEUS detector can be found elsewhere [14, 15]. A brief outline of the components most relevant for this analysis is given below.

---

[1] Hereafter, the positron is referred to with the same symbol, e, as the electron.

[2] The data taking period between 1995 and 2000 is referred to a HERA I, while the period 2002-2007 is referred to as HERA II

Charged particles were tracked in the Cetral Tracking Detector (CTD) [16] and, in the HERA II period, also in the Micro Vertex Detector (MVD). These components operated in a magnetic field of 1.43 T provided by a superconductong thin solenoid. The CTD consisted of 72 cylindrical drift-chamber layers, organised in nine superlayers covering the polar-angle [3] region $15^\circ < \theta < 164^\circ$. The transverse-momentum resolution for full-length tracks was $\sigma(p_T)/p_T = 0.0058 p_T \oplus 0.0065 \oplus 0.0014/p_T$, with p_T in GeV.

The MVD consisted of a barrel (BMVD) and a forward (FMVD) section with three cylindrical layers and 4 vertical planes of single-sided silicon strip sensors in the BMVD and FMVD respectively. The BMVD extended the polar-angle coverage for tracks with three measurements from 30° to 50°. The FMVD extended the polar-angle coverage in the forward region to 7°.

The uranium–scintillator calorimeter (CAL) [17] covered 99.7% of the total solid angle and consisted of three parts: the forward (FCAL), the barrel (BCAL) and the rear (RCAL) calorimeters. Each part was subdivided transversely into towers and longitudinally into one electromagnetic section (EMC) and either one (in RCAL) or two (in BCAL and FCAL) hadronic sections (HAC). The CAL energy resolutions, as measured under test-beam conditions, were $\sigma(E)/E = 0.18/\sqrt{E}$ for positrons and $\sigma(E)/E = 0.35/\sqrt{E}$ for hadrons, with E in GeV.

The position of positrons scattered at small angles with respect to the positron-beam direction was determined combining the information from the CAL, the small-angle rear tracking detector (SRTD) and the hadron-electron separator (HES) [18, 19].

The FPC [20] was used in HERA I to measure the energy of particles in the pseudorapidity range $\eta \approx 4.0 - 5.0$. It consisted of a lead–scintillator sandwich calorimeter installed in the 20×20 cm^2 beam hole of the FCAL. The energy resolution for electrons, as measured in a test beam, was $\sigma(E)/E = (0.41 \pm 0.02)/\sqrt{E} \oplus 0.062 \pm 0.002$, with E in GeV. The energy resolution for pions was $\sigma(E)/E = (0.65 \pm 0.02)/\sqrt{E} \oplus 0.06 \pm 0.01$, with E in GeV, after having combined the information from FPC and FCAL. The e/h ratio was close to unity.

The acceptance and the detector response were determined using Monte Carlo (MC) simu-

[3] The ZEUS coordinate system is a right-handed Cartesian system, with the Z axis pointing in the proton direction, referred to as the "forward direction", and the X axis pointing left towards the centre of HERA. The coordinate origin is at the nominal interaction point. The pseudorapidity is defined as $\eta = -\ln(\tan\frac{\theta}{2})$, where the polar angle θ is measured with respect to the proton beam direction.

lations. The detector was simulated in detail using a program based on GEANT 3.13 [21]. All the simulated events were processed through the same reconstruction and analysis chain as the data.

A MC generator, GENDVCS [22], based on a model by Frankfurt, Freund and Strikman (FFS) [23], was used to simulate the elastic DVCS process as described in [24]. The ALLM97 [25] parameterisation of the F_2 structure function of the proton was used as input. The t dependence was assumed to be exponential with a slope parameter b set to 4.5 GeV^{-2}, independent of W and Q^2.

The elastic, $ep \to e\gamma p$, and inelastic, $ep \to e\gamma Y$, BH processes, where Y is the hadronic final state, and the exclusive dilepton production, $ep \to ee^+e^-p$, were simulated using the GRAPE-COMPTON[4] [26] and the GRAPE-DILEPTON [26] generators. These two MC programs are based on the automatic system GRACE [27] for calculating Feynman diagrams. A possible contribution from vector meson electroproduction was simulated with the ZEUSVM generator [28]. To account for electroweak radiative effects, all the generators were interfaced to HERACLES 4.6 [29].

3 Kinematic variables and event selection

The process $ep \to e\gamma p$ is parametrised by the following variables:

- $Q^2 = -q^2 = -(k - k')^2$, the negative four-momentum squared of the virtual photon, where k (k') is the four-momentum of the incident (scattered) positron;
- $W^2 = (q + p)^2$, the squared centre-of-mass energy of the photon-proton system, where p is the four-momentum of the incident proton;
- $x = Q^2/(2P \cdot q)$, the fraction of the proton momentum carried by the quark struck by the virtual photon in the infinite-momentum frame (the Bjorken variable);
- $x_L = \frac{p' \cdot k}{p \cdot k}$, the fractional momentum of the outgoing proton, where p' is the four-momentum of the scattered proton;
- $t = (p - p')^2$, the squared four-momentum transfer at the proton vertex.

For the Q^2 range of this analysis and at small values of t, the signature of elastic DVCS and BH events consists of a scattered positron, a photon and a scattered proton. The scattered

[4] Hereafter, the GRAPE-COMPTON generator is referred to as GRAPE.

proton remains in the beam-pipe. The events were selected online via a three-level trigger system [14,30]. The trigger required events to contain two isolated electromagnetic (EM) clusters with energy greater than 2 GeV.

The offline selection followed the same strategy as for a previous publication [24]. Two EM clusters were found by a dedicated, neural-network based, positron finder [31]. They were ordered in polar angle and are in the following denoted as EM1 and EM2, with $\theta_1 > \theta_2$. The first cluster was required to be in the RCAL with energy $E_1 > 10\,\text{GeV}$; the second cluster had to have a polar angle $\theta_2 < 2.85\,\text{rad}$ and was required to be either in the RCAL, with energy $E_2 > 3\,\text{GeV}$, or in the BCAL, with energy $E_2 > 2.5\,\text{GeV}$. The angular range of the second cluster corresponds to the region of high reconstruction efficiency for tracks in the CTD. The association of a track discriminates between positron and photon induced clusters. For events with one track, a match was required between the track and one of the two EM clusters. Events with more than one track were rejected. In order to ensure a uniform high acceptance for the electromagnetic cluster in the RCAL some fiducial cuts were required on the position of the electromagnetic cluster on the RCAL surface. A different fiducial cut was applied in the HERA I and HERA II analyses, due to the different RCAL detector acceptance.

The condition $40 < E - P_Z < 70$ GeV was imposed, with $E = E_1 + E_2$ and $P_Z = E_1 \cos\theta_1 + E_2 \cos\theta_2$. This requirement rejected photoproduction events and also events in which a hard photon was radiated from the incoming positron.

Events with CAL energy deposits not associated with the two EM clusters were rejected if their energy was above the noise level in the CAL [32]. In addition, the total energies measured in the FPC (only for HERA I) and in the FCAL were each required to be below 1 GeV. These elasticity requirements also suppressed DVCS events and inelastic BH events in which the proton dissociates into a high-mass hadronic system. The sample was still contaminated by events in which a forward, low-mass hadronic system was not visible in the main detector.

For HERA I, the kinematic region was $40 < W < 170\,\text{GeV}$ and $1.5 < Q^2 < 100\,\text{GeV}^2$. In the HERA II analysis, the minimum Q^2 cut was raised to $5\,\text{GeV}^2$. The HERA I restricted sample consisted of HERA I data with the same box and kinematic cuts of HERA II. For the purposes of this analysis, the values of Q^2 and W were determined for each event, independently of its topology, under the assumption that the EM1 cluster is the scattered positron. This assumption is always valid for DVCS events for the Q^2 range considered here. The electron method [33] was used to determine Q^2 and the double-angle method [33] to determine W.

4 Background study and signal extraction

The selected events were subdivided into three samples:

- γ sample: EM2, with no track pointing to it, is taken to be the photon and EM1 is assumed to be the scattered positron. Both BH and DVCS processes contribute to this topology. The sample consisted of 7618 events for HERA I, 6315 for HERA II and 3368 for the HERA I restricted sample.
- e sample: EM2, with a positive-charge track pointing to it, is assumed to be the scattered positron and EM1 is the photon. The sample is dominated by BH events. The number of DVCS events is predicted to be negligible due to the large Q^2 implied by the large positron scattering angle. This sample consisted of 11988 events for HERA I, 10198 for HERA II and 5385 for the HERA I restricted sample.
- negative-charge-e sample: EM2, with a negative-charge track pointing to it, may have originated from an e^+e^- final state accompanying the scattered positron, where one of the positrons escaped detection. This sample is dominated by non-resonant e^+e^- production and by J/ψ production with subsequent decay into e^+e^- and was used to study these background sources. It consisted of 764 events for HERAI, 391 for HERA II and 195 for the HERA I restricted sample. The contribution from diffractive electroproduction of ρ, ω and ϕ mesons was found to be negligible [24].

In the kinematic region of this analysis, the contribution of the interference term between the DVCS and BH amplitudes is very small when the cross section is integrated over the angle between the positron and proton scattering planes [34, 35]. Thus the cross section for exclusive production of real photons was treated as a simple sum over the contributions from the DVCS and BH processes. The DVCS cross section was determined by subtracting the latter.

The size of the BH contribution to be subtracted was determined using the e sample which consists of elastic and inelastic BH events and a small fraction of exclusive e^+e^- production. The exclusive e^+e^- contribution was estimated with the negative-charge-e sample to be $(6.4 \pm 0.3)\%$ for HERA I, $(3.8 \pm 0.3)\%$ for HERA II and subtracted from the e sample.

The measured cross section of the BH process was $(4 \pm 1)\%$ smaller than the expectations of the GRAPE program (a detailed discussion can be found elsewhere [36,37]). The GRAPE cross section was modified accordingly.

The BH contribution to the γ sample was determined by GRAPE and found to be $(56 \pm 1)\%$ for HERA I and $(58 \pm 1)\%$ for HERA II. The BH-subtracted γ sample was further scaled by $(1 - f_{p-\mathrm{diss}})$, where $f_{p-\mathrm{diss}}$ is the fraction of DVCS events in which the proton dissociated into a low-mass state. Its value was taken [24] from a previous publication [38], $f_{p-\mathrm{diss}} = 17.5 \pm 1.3^{+3.7}_{-3.2}\%$.

The W and Q^2 distributions separately for the e sample, for the γ sample and for the γ sample after BH and proton dissociation background subtraction, for both HERA I and HERA II, are shown in Fig. 1. Also shown in the figure are the MC expectations which describe the data well. In Fig. 2 the shape comparison between the HERA I and HERA II data is shown for the γ sample in the same phase space region and using the same selection cuts.

5 Results

The $\gamma^* p$ cross section of the DVCS process was calculated as a function of W and Q^2 using the formula

$$\sigma^{\gamma^* p \to \gamma p}(W_i, Q_i^2) = \frac{(N_i^{\mathrm{obs}} - N_i^{\mathrm{BH}}) \cdot (1 - f_{p-\mathrm{diss}})}{N_i^{\mathrm{MC}}} \cdot \sigma^{\mathrm{FFS}(\gamma^* p \to \gamma p)}(W_i, Q_i^2),$$

where N_i^{obs} is the total number of data events in the γ sample in each bin i of W and Q^2, N_i^{BH} denotes the number of elastic and inelastic BH events in the γ sample in the same bin, and N_i^{MC} is the number of events expected in the γ sample from GENDVCS for the luminosity of the data. The cross section as predicted by the FFS model is denoted as $\sigma^{\mathrm{FFS}}(\gamma^* p \to \gamma p)$ and was evaluated at the centre (W_i, Q_i^2) of each Q^2 and W bin. The $\gamma^* p$ DVCS cross section, $\sigma^{\gamma^* p \to \gamma p}$, is shown in Fig. 3 as a function of Q^2 at $W = 104$ GeV and as a function of W at $Q^2 = 3.2$ GeV^2. The cross section shows a fast decrease with Q^2. The figure shows the perfect agreement between this analysis and the analysis that is going to be published.The points coming from my analysis, have been shifted for clarity. A fit to the Q^2 and W dependence of the cross sections, assuming the functional forms $\sigma^{\gamma^* p \to \gamma p}(Q^2) \sim Q^{-2n}$ and $\sigma^{\gamma^* p \to \gamma p}(W) \sim W^{\delta}$, was performed for $W = 104$ GeV and for $Q^2 = 3.2$ GeV^2,respectively. Figure 4-5-6 show the result of the fit on the HERA I, HERA

II aand the HERA I restricted sample cross sections. The result are in good agreement. The improvement in the statistical precision obtained using HERA II data is evident. The result is in agreement with other DVCS measurements at HERA at lower W [24, 39–41]. As expected for DVCS [23], the decrease of the cross section with Q^2 is slower than for exclusive vector meson production [9–13, 42]. The cross section increases with W. In pQCD-based models, this behaviour is related to the increase of the gluon content of the proton with decreasing Bjorken-x. This result is in agreement with the previous measurements [24, 39–41] performed in a restricted range of W and at higher Q^2. The numbers of DVCS events, together with the respective BH percentage and luminosity, are listed in Table 2 1. This number scales with the luminosity, as expected. This means that considering all the HERA II running period, where the collected luminosity was 400 pb^{-1}, for the future analysis we can start with $6815 * 400/41 = 7611$ events of a pure DVCS sample.This number can be increased with a better tuning of the cuts for the HERA II enviroment, a better understanding of the different background components and the use of the MVD for both backgound and signal. This increase of statistics looks promising in order to perform a new measurement of $d\sigma/dt$ using the HERA II data with larger statistics and therefore better precision.

6 Conclusion and Outlook

Repeating the analysis of the HERA I data that will be published soon, we have verified that, varying only the box cuts and kinematic region of the HERA I selection, we can obtain a measurement of the DVCS cross section with the HERA II data compatible with the previous measurements. The increase of statistic in the HERA II analysis has opened the way to a future study of $d\sigma/dt$ where t will be calculated in a indirect way using the expression

$$t = -p_x'^2 - p_y'^2 = -p_T'^2 = -(\gamma_T' + e_T')^2$$

which needs a high resolution on both e_T' and γ_T'. However for a complete analysis we need a better tuning of the cuts for the HERA II environment, a better understanding of the different background components and Monte Carlo studies both to define the new kinematic region and the resolution study of the variables in th new data taking period.

7 Acknowledgements

This experience was strongly formative because it has allowed me to be an active part of a collaboration, in parallel with high-level courses. In the collaboration I felt welcome and thanks to this I could give a first look to a very interesting and complicate analysis, studying the DVCS process with both the HERA I and HERA II data. I would like to thank first of all my great supervisors Enrico and Marcella for the availability and the encouragement they have always given to me. The time I spent working with them was very hard and...nice! This was the best time here in DESY. I want also to thank the Italian Group for their help, patience and coffee. In particular my best thanks are for Monica and Silvia who always have time for me. Their help and support were indispensable to proceed during this period. A particular thank goes moreover to Justyna who has always been available to clarify my doubts and to give me material for the analysis. All these people are wonderful and I hope to see them again as soon as possible.Many thanks to Mr. Meyer, Mrs. Schrader and Ingrid for the organization of the SummerSchool, that has been the best summer of my life.

References

[1] M. Diehl, T. Gousset, B. Pire and J. Ralston, Phys. Lett. **B 411**, 193 (1997).

[2] M. Burkardt, Int. J. Mod. Phys. **A 18**, 173 (2003).

[3] M. Diehl, Eur. Phys. J. **C 25**, 223 (2002).

[4] V. Guzey and T. Teckentrup, Phys. Rev. **D 74**, 54027 (2006).

[5] K. Kumerički, Nucl. Phys. **B 794**, 223 (2008).

[6] ZEUS Coll., J. Breitweg et al., Phys. Lett. **B 487**, 273 (2000).

[7] ZEUS Coll., S. Chekanov et al., Nucl. Phys. **B 718**, 2 (2005).

[8] ZEUS Coll., S. Chekanov et al., Nucl. Phys. **B 695**, 3 (2004).

[9] ZEUS Coll., J. Breitweg et al., Eur. Phys. J. **C 14**, 213 (2000).

[10] H1 Coll., C. Adloff et al., Phys. Lett. **B 483**, 360 (2000).

[11] ZEUS Coll., S. Chekanov et al., PMC Phys. **A 1**, 6 (2007).

[12] H1 Coll., A. Aktas et al., Eur. Phys. J. **C 46**, 585 (2006).

[13] H1 Coll., C. Adloff et al., Eur. Phys. J. **C 13**, 371 (2000).

[14] ZEUS Coll., U. Holm (ed.), *The ZEUS Detector*. Status Report (unpublished), DESY (1993), available on `http://www-zeus.desy.de/bluebook/bluebook.html`.

[15] ZEUS Coll., M. Derrick et al., Phys. Lett. **B 293**, 465 (1992).

[16] N. Harnew et al., Nucl. Inst. Meth. **A 279**, 290 (1989);
B. Foster et al., Nucl. Phys. Proc. Suppl. **B 32**, 181 (1993);
B. Foster et al., Nucl. Inst. Meth. **A 338**, 254 (1994).

[17] M. Derrick et al., Nucl. Inst. Meth. **A 309**, 77 (1991);
A. Andresen et al., Nucl. Inst. Meth. **A 309**, 101 (1991);
A. Caldwell et al., Nucl. Inst. Meth. **A 321**, 356 (1992);
A. Bernstein et al., Nucl. Inst. Meth. **A 336**, 23 (1993).

[18] A. Bamberger et al., Nucl. Inst. Meth. **A 401**, 63 (1997).

[19] A. Dwurazny et al., Nucl. Inst. Meth. **A 277**, 176 (1989).

[20] ZEUS Coll., FPC group, A. Bamberger et al., Nucl. Inst. Meth. **A 450**, 235 (2000).

[21] R. Brun et al., *GEANT3*. Technical Report CERN-DD/EE/84-1,CERN, 1987.

[22] P.R.B. Saull, *A Monte Carlo Generator for Deeply Virtual Compton Scattering at HERA*, 1999, available on `http://www-zeus.desy.de/physics/diff/pub/MC`.

[23] L.L. Frankfurt, A. Freund and M. Strikman, Phys. Rev. **D 58**, 114001 (1998). Erratum-ibid **D 59** (1999) 119901.

[24] ZEUS Coll., S. Chekanov et al., Phys. Lett. **B 573**, 46 (2003).

[25] H. Abramowicz and A. Levy, Preprint DESY-97-251 (hep-ph/9712415), DESY, 1997.

[26] T. Abe, Comp. Phys. Comm. **136**, 126 (2001).

[27] T. Ishikawa et al., *GRACE manual: Automatic generation of tree amplitudes in Standard Models: Version 1.0.* KEK Report 92-19, 1993.

[28] K. Muchorowski, Ph.D. Thesis, Warsaw University, 1998 (unpublished).

[29] H. Spiesberger, *An Event Generator for ep Interactions at HERA Including Radiative Processes (Version 4.6)*, 1996, available on `http://www.desy.de/~hspiesb/heracles.html`.

[30] W.H. Smith, K. Tokushuku and L.W. Wiggers, *Proc. Computing in High-Energy Physics (CHEP),* Annecy, France, Sept. 1992, C. Verkerk and W. Wojcik (eds.), p. 222, CERN, Geneva, Switzerland (1992). Also in preprint DESY 92-150B.

[31] H. Abramowicz, A. Caldwell and R. Sinkus, Nucl. Inst. Meth. **A 365**, 508 (1995); R. Sinkus and T. Voss, Nucl. Inst. Meth. **A 391**, 360 (1997).

[32] R. Ciesielski, *Exclusive J/Psi Production in Deep Inelastic ep Scattering in the ZEUS exeriment at HERA.* Ph.D. Thesis, Warsaw University, Warsaw, Poland, 2004.

[33] S. Bentvelsen, J. Engelen and P. Kooijman, *Proc. Workshop on Physics at HERA*, W. Buchmüller and G. Ingelman (eds.), Vol. 1, p. 23, Hamburg, Germany, DESY (1992);
K.C. Höger, ibid, p.43.

[34] L. Frankfurt, A. Freund and M. Strikman, Phys. Lett. **B 460**, 417 (1999).

[35] A.V. Belitsky, D. Müller and A. Kirchner, Nucl. Phys. **B 629**, 323 (2002).

[36] I. Grabowska-Bołd, *Measurement of Deeply Virtual Compton Scattering Using the ZEUS Detector at HERA.* Ph.D. Thesis, University of Mining and Metallurgy, Cracow, Poland, Report DESY-THESIS-2004-034, 2003.

[37] S. Fazio, *Measurement of Deeply Virtual Compton Scattering cross sections at HERA and a new model for the DVCS amplitude.* Ph.D. Thesis, Calabria University, Rende (Cosenza), Italy, 2007, available on `http://www-zeus.desy.de/physics/diff/pub/theses.html`.

[38] ZEUS Coll., S. Chekanov et al., Eur. Phys. J. **C 24**, 345 (2002).

[39] H1 Coll., C. Adloff et al., Phys. Lett. **B 517**, 47 (2001).

[40] H1 Coll., A. Aktas et al., Eur. Phys. J. **C 44**, 1 (2005).

[41] H1 Coll., F.D. Aktas et al., Phys. Lett. **B 659**, 796 (2008).

[42] ZEUS Coll., J. Breitweg et al., Eur. Phys. J. **C 6**, 603 (1999).

Samples	DVCS events	BH (%)
HERA I (pub.)	3328	56.3±1.0
HERA I ($Q^2 > 5\text{GeV}^2$)	1233	63.4±1.1
HERA II (06-07)	2746	56.5±1.1

Table 1: *The sample of DVCS events after BH the background subtraction, the sample still include the proton dissociative contribute. The last coloumn indicate the BH fraction subtracted.*

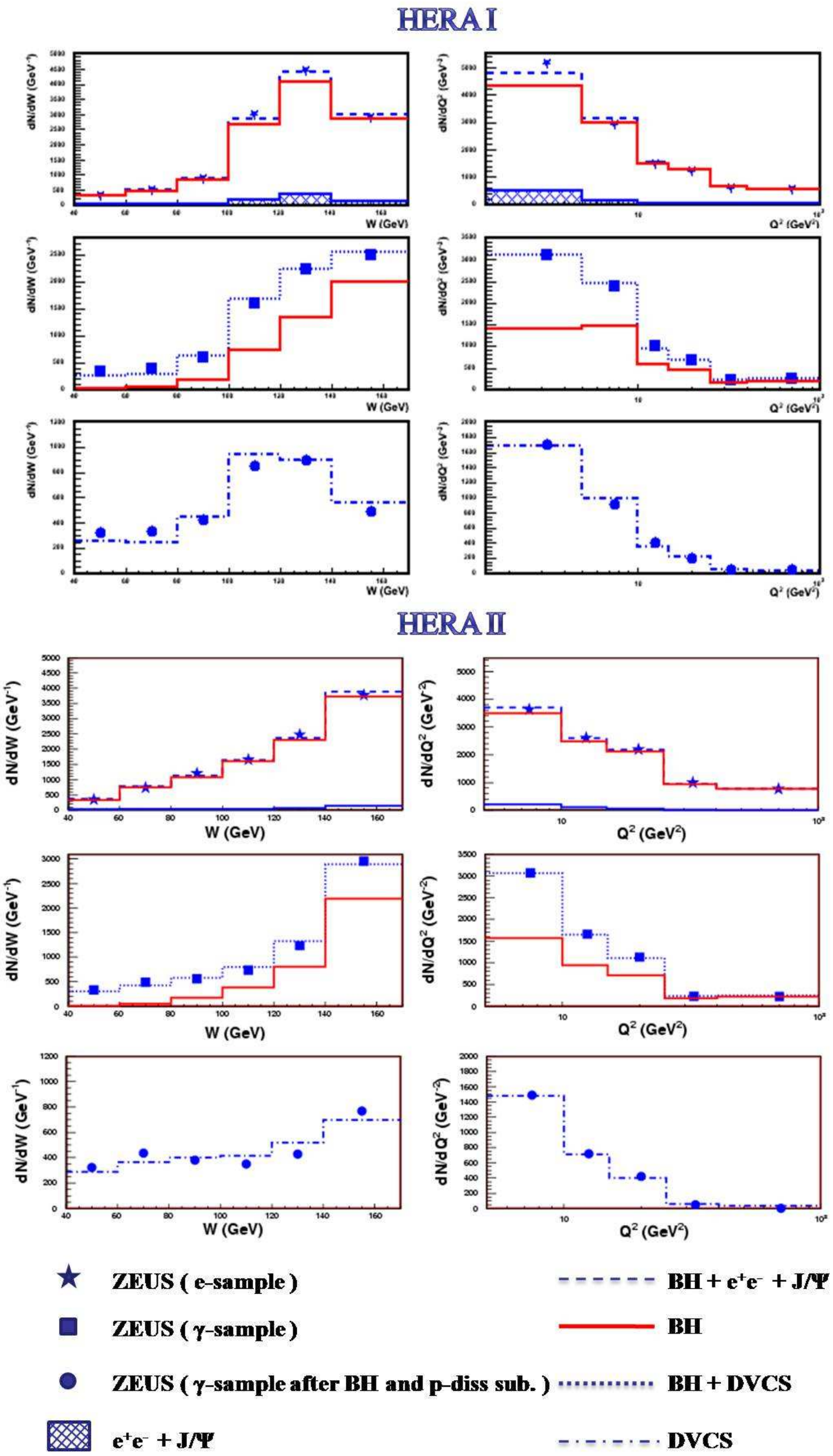

Figure 1: *Distribution of W, Q^2 in the inclusive sample for HERA I and HERA II, for the e-sample (top), the γ-sample (middle) and the γ-sample after BH background and proton dissociation subtraction (bottom). Also shown are the expectations of the MC normalised to the luminosity of the data and the contribution from exclusive dilepton production (e^+e^-).*

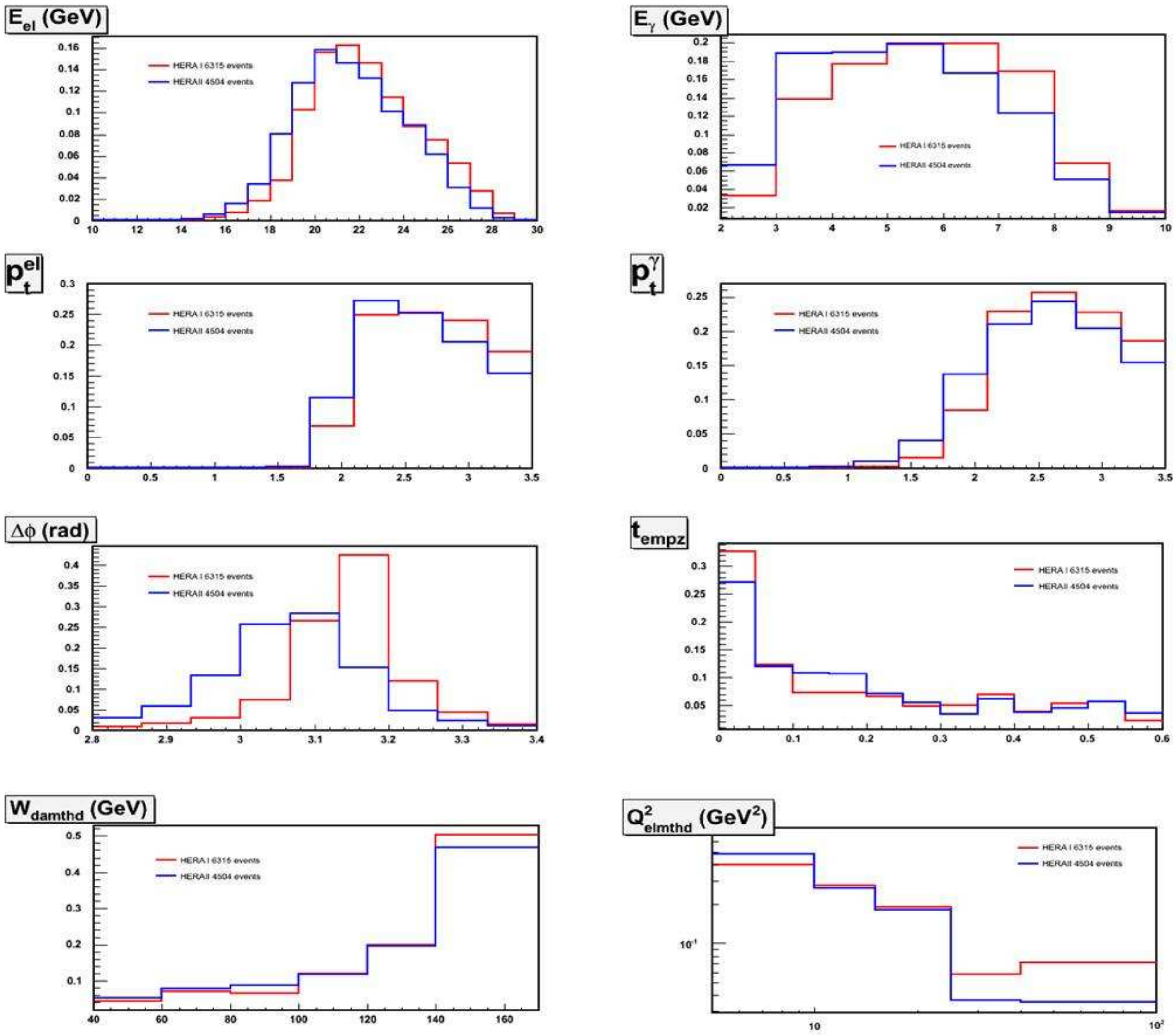

Figure 2: *Shape comparison between the HERA I and the HERA II data within the same phase space region and using the same selection cuts*

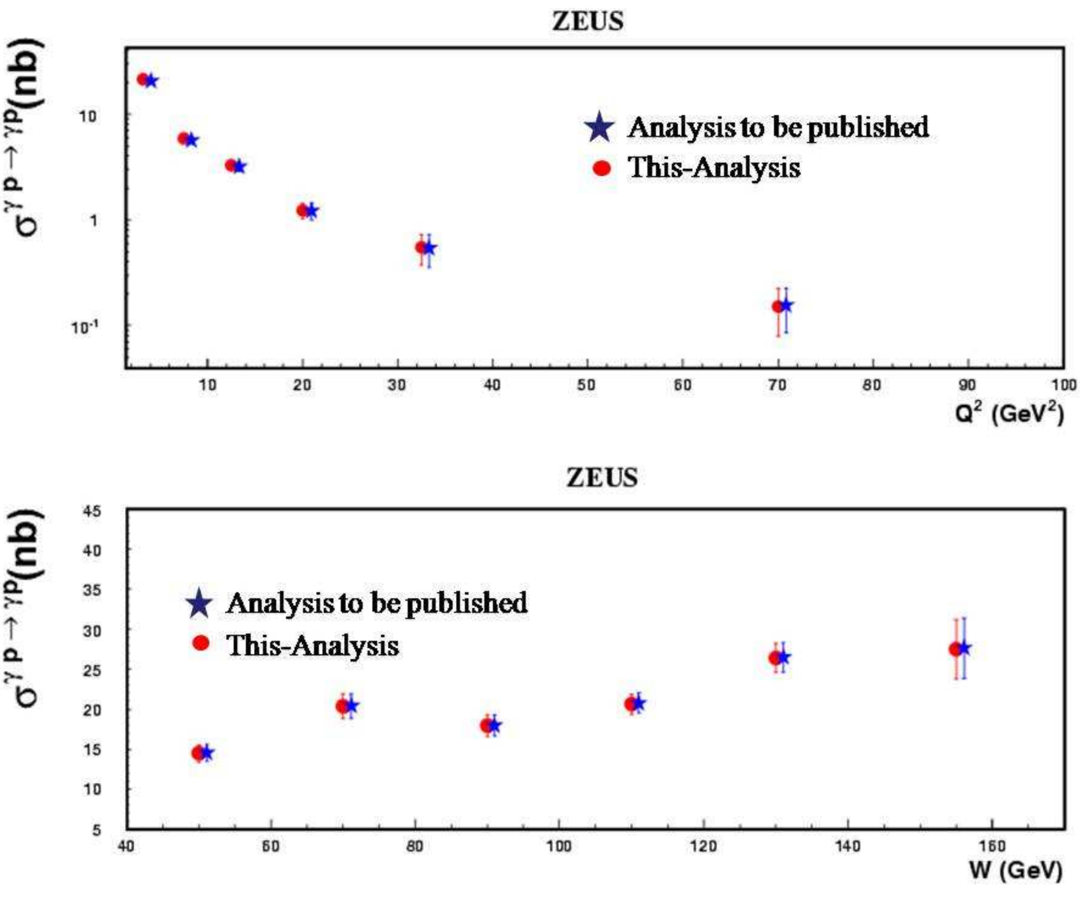

Figure 3: *(top) The DVCS cross section, $\sigma^{\gamma^* p \to \gamma p}$, as a function of Q^2 for both this analysis and the analysis to be published. (bottom) The DVCS cross section, $\sigma^{\gamma^* p \to \gamma p}$, as a function of W for both this analysis and the analysis to be published. The points of this analysis have been shifted for more clarity.*

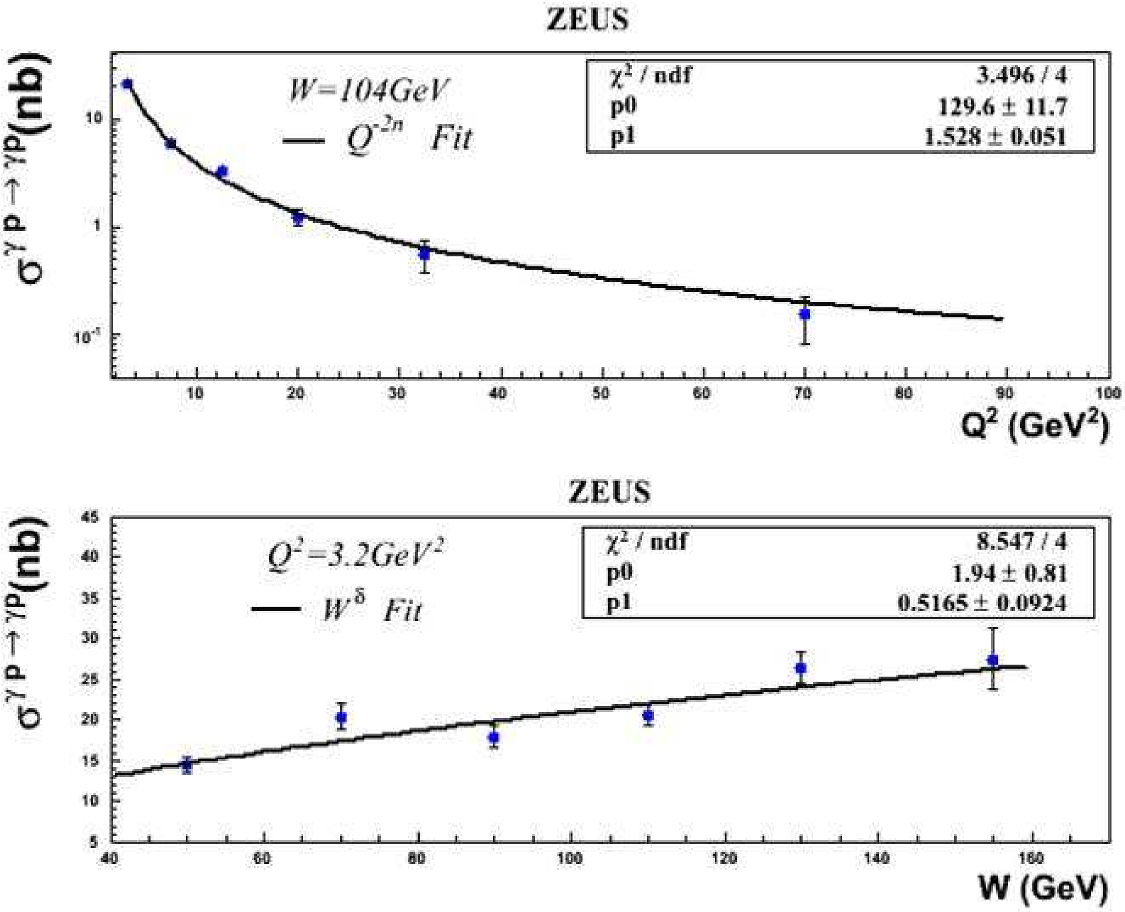

Figure 4: *Fit to $d\sigma/dQ^2$ and $d\sigma/dW$,assuming the functional form Q^{-2n} and W^{δ}.The cross sections were obtained using the HERA I data and in the same kinematic region as for the analysis to be published.*

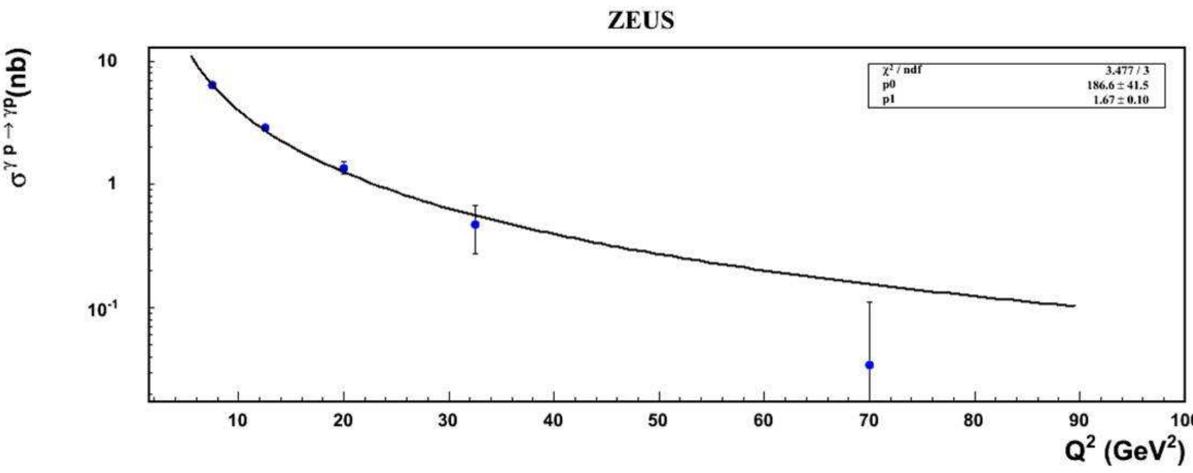

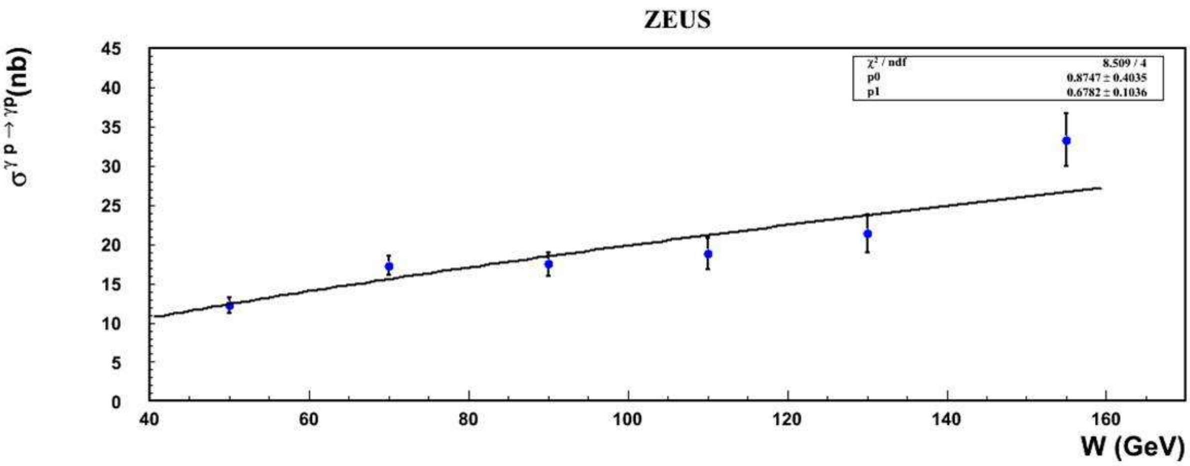

Figure 5: *Fit to $d\sigma/dQ^2$ and $d\sigma/dW$,assuming the functional form Q^{-2n} and W^{δ}.The cross sections were obtained using the HERA II data in the restricted kinematic region described in the text.*

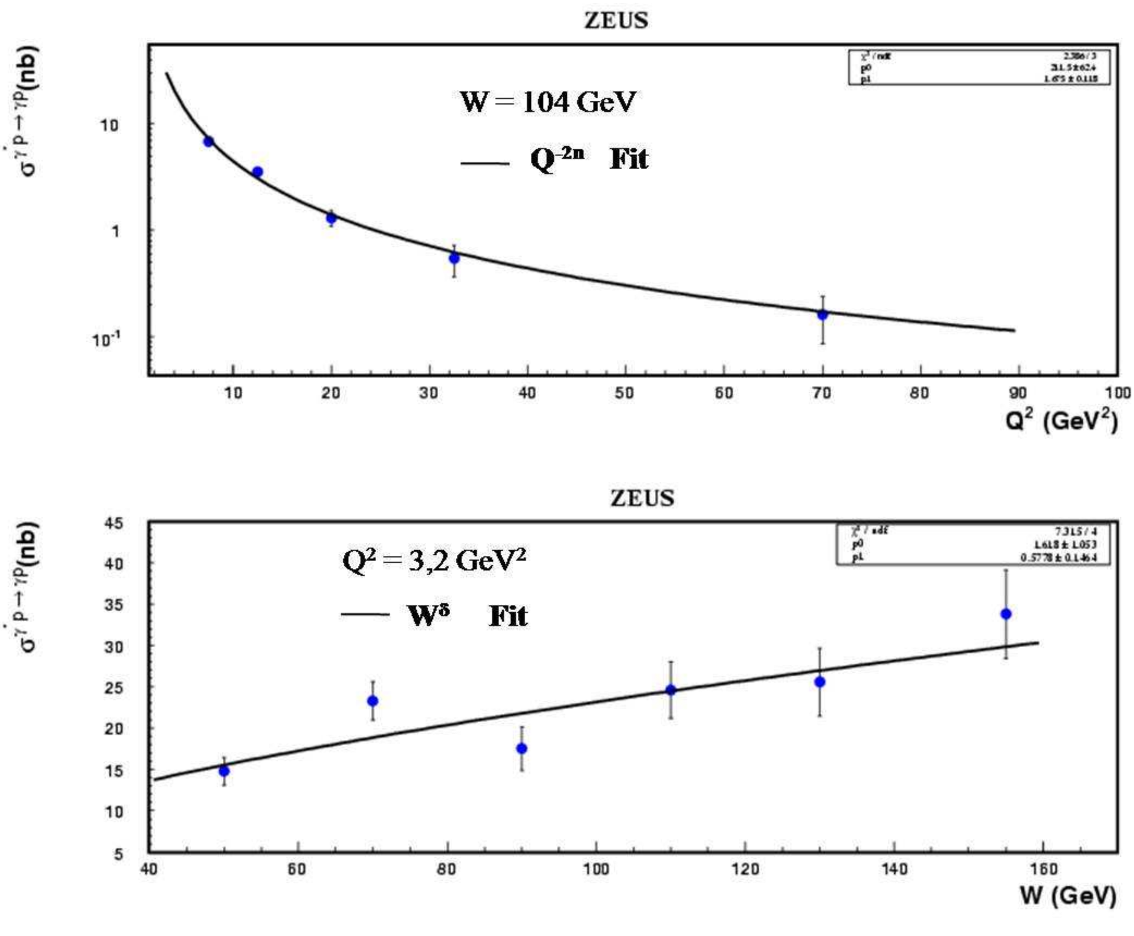

Figure 6: *Fit to $d\sigma/dQ^2$ and $d\sigma/dW$,assuming the functional form Q^{-2n} and W^{δ}.The cross sections were obtained using the HERA I data in the restricted kinematic region described in the text.*